



## Molecular Crystals and Liquid Crystals

Publication details, including instructions for authors and subscription information:

<http://www.tandfonline.com/loi/gmcl20>

### New Organic Conductor Based on Tetrathiapentalene Derivative (BDA-TTP)<sub>4</sub>Hg<sub>2</sub>I<sub>6</sub>

E. I. Zhilyaeva<sup>a</sup>, A. M. Flakina<sup>a</sup>, E. I. Yudanova<sup>a</sup>,  
R. N. Lyubovskaya<sup>a</sup>, I. V. Fedyanin<sup>b</sup>, K. A.  
Lyssenko<sup>b</sup> & J. Yamada<sup>c</sup>

<sup>a</sup> Institute of Problems of Chemical Physics RAS,  
Chernogolovka, Russia

<sup>b</sup> Nesmeyanov Institute of Organoelement  
Compounds RAS, Moscow, Russia

<sup>c</sup> University of Hyogo, Kamigori-cho, Hyogo, Japan

Version of record first published: 22 Sep 2010

To cite this article: E. I. Zhilyaeva, A. M. Flakina, E. I. Yudanova, R. N. Lyubovskaya, I. V. Fedyanin, K. A. Lyssenko & J. Yamada (2007): New Organic Conductor Based on Tetrathiapentalene Derivative (BDA-TTP)<sub>4</sub>Hg<sub>2</sub>I<sub>6</sub>, Molecular Crystals and Liquid Crystals, 468:1, 151/[503]-161/[513]

To link to this article: <http://dx.doi.org/10.1080/15421400701229818>

PLEASE SCROLL DOWN FOR ARTICLE

Full terms and conditions of use: <http://www.tandfonline.com/page/terms-and-conditions>

This article may be used for research, teaching, and private study purposes. Any substantial or systematic reproduction, redistribution, reselling, loan,

sub-licensing, systematic supply, or distribution in any form to anyone is expressly forbidden.

The publisher does not give any warranty express or implied or make any representation that the contents will be complete or accurate or up to date. The accuracy of any instructions, formulae, and drug doses should be independently verified with primary sources. The publisher shall not be liable for any loss, actions, claims, proceedings, demand, or costs or damages whatsoever or howsoever caused arising directly or indirectly in connection with or arising out of the use of this material.



## New Organic Conductor Based on Tetrathiapentalene Derivative (BDA-TTP)<sub>4</sub>Hg<sub>2</sub>I<sub>6</sub>

**E. I. Zhilyaeva**

**A. M. Flakina**

**E. I. Yudanov**

**R. N. Lyubovskaya**

Institute of Problems of Chemical Physics RAS, Chernogolovka, Russia

**I. V. Fedyanin**

**K. A. Lyssenko**

Nesmeyanov Institute of Organoelement Compounds RAS,  
Moscow, Russia

**J. Yamada**

University of Hyogo, Kamigori-cho, Hyogo, Japan

*New radical cation salt BDA-TTP [2,5-bis(1,3-dithian-2-ylidene)-1,3,4,6-tetrathiapentalene] with iodo-mercurate anion of the (BDA-TTP)<sub>4</sub>Hg<sub>2</sub>I<sub>6</sub> composition has been synthesized. X-ray analysis at 100 K revealed the alternation of conducting donor layers of the  $\beta$ -type and inorganic layers composed of the [Hg<sub>2</sub>I<sub>6</sub>]<sup>2-</sup> anions. The compound shows a semiconducting temperature dependence of resistivity and the temperature activation dependence of spin susceptibility.*

**Keywords:** electrical conductivity; radical cation salts; X-ray diffraction

## INTRODUCTION

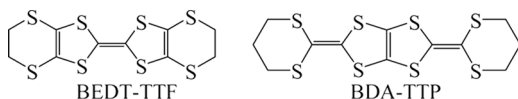
Most of organic conductors synthesized by now are based on tetrathiafulvalene derivatives [1,2]. Mercury halides were found to form anions of various composition and structure in radical cation salts of bis(ethylenedithio)tetrathiafulvalene (BEDT-TTF) and its analogs [3], which

The work was supported by the Russian Foundation for Basic Research (grant #04-03-32296a).

Address correspondence to E. I. Zhilyaeva, Institute of Problems of Chemical Physics RAS, Chernogolovka, 142432, Russia. E-mail: zhilya@icp.ac.ru

affect the structure of conducting organic layers and electroconducting properties of the compounds. In particular, the radical cation salts  $(\text{BEDT-TTF})_4\text{Hg}_{2.89}\text{Br}_8$  [4],  $(\text{BEDT-TTF})_4\text{Hg}_{2.78}\text{Cl}_8$  [5],  $(\text{BETS})_4\text{Hg}_{2.84}\text{Br}_8$  [6] и  $(\text{EDT-TTF})_4[\text{Hg}_3\text{I}_8]_{1-x}$  [7] are characterized by polymeric structures of anions and undergo a superconducting transition upon cooling.

Recently, it has been found that the BDA-TTP [2,5-bis(1,3-dithian-2-ylidene)-1,3,4,6-tetrathiapentalene] donor, which belongs to the family different from the BEDT-TTF one, namely, the 1,3,4,6-tetrathiapentalene family, forms organic superconductors with the  $\text{SbF}_6^-$ ,  $\text{AsF}_6^-$ , and  $\text{PF}_6^-$  anions and is promising to be used in syntheses of new organic conductors [8]. Thus, it was of interest to synthesize radical cation salts of BDA-TTP with halomercurate anions and study their electroconducting properties.



Recently [9] we have prepared the radical cation salts of BDA-TTP with bromo- and iodomercurate anions of the  $(\text{BDA-TTP})_4\text{Hg}_2\text{Br}_6$  and  $(\text{BDA-TTP})_6\text{Hg}_4\text{I}_{10.34}$  compositions. The salts are composed of the  $\beta$ -type conducting organic layers and the dimerized  $[\text{Hg}_2\text{Br}_6]^{2-}$  and  $[\text{Hg}_4\text{I}_{10.34}]^{2.34-}$  anions. The present article reports on the synthesis of the new radical cation salt of BDA-TTP with the iodomercurate anion,  $(\text{BDA-TTP})_4\text{Hg}_2\text{I}_6$  (**1**), and the study of its crystal structure at 100 K, conductivity, and ESR spectra.

## EXPERIMENTAL PROCEDURE

$\text{Bu}_4\text{NHgI}_3$  was synthesized according to the procedure described in [10]. The crystals of **1** were obtained by electrochemical oxidation of BDA-TTP at 20°C and current of 0.5  $\mu\text{A}$ . The 0.5 mm thick Pt wire was used as an anode, and the 0.3 mm thick molybdenum wire was used as a cathode. BDA-TTP (8.2 mg, 2 mmol) dissolved in 3 ml of chlorobenzene was placed in the anodic chamber of the cell, the solution of  $\text{HgI}_2$  (23 mg, 0.05 mmol) and  $\text{Bu}_4\text{NHgI}_3$  (82.4 mg 0.1 mmol) in the chlorobenzene (5 ml)/dehydrated ethanol (0.8 ml) mixture was added to both cathode and anode compartments to level both sides. After seven days, the crystals of the  $\text{BDA-TTP}_6\text{Hg}_4\text{I}_{10.34}$  (**2**) composition described by us earlier in [9] were peeled off from the anode. The crystals appeared as sharp edged plates. After that, the

electrocrystallization process was carried out for ten days in similar conditions to yield the crystals of **1** as bars.

Resistivity of single crystals was measured from 300 down to 140 K by a standard *dc* four-probe technique with graphite paste.

The ESR spectra of the single crystals were recorded on a RADIO-PAN SE/X-2547 spectrometer with 100 kHz magnetic modulation and a maximum value of microwave power 100 mW equipped with a Radiopan TC-660 and RR-221 cryostat system. A single crystal was put in the center of a quartz ampoule. The ESR line shape was close to the Lorentzian line that allowed us to estimate paramagnetic susceptibility of the crystal from the integral intensity of the ESR spectrum.

At  $T = 100$  K the crystals of  $C_{48}H_{48}S_{16}Hg_2I_8$  ( $0.37 \times 0.24 \times 0.10$  mm) are triclinic, space group  $P\bar{1}$ ,  $a = 11.9799(7)$ ,  $b = 17.729(1)$ ,  $c = 20.277(1)$  Å,  $\alpha = 105.100(1)$ ,  $\beta = 100.097(1)$ ,  $\gamma = 106.507(1)^\circ$ ,  $V = 3839.3(4)$  Å<sup>3</sup>,  $Z = 2$  ( $Z' = 1$ ),  $d_{calc} = 2.434$  g/cm<sup>-3</sup>,  $F(000) = 2652$ . The intensities of 47063 reflections were measured at 100 K on an APEX II CCD diffractometer ( $\lambda(MoK\alpha) = 0.71072$  Å, graphite monochromator,  $\omega$ -scanning,  $2\theta < 58^\circ$ ), and 20369 independent reflections ( $R_{int} = 0.0347$ ) were used in the refinement. Absorption ( $\mu = 73.13$  cm<sup>-1</sup>) was accounted for using the real shape of the crystal. The structure was solved by a direct method and refined by the full-matrix least-squares technique against  $F_{hkl}^2$  with the anisotropic thermal parameters for all non-hydrogen atoms. The positions of hydrogen atoms were calculated geometrically and refined by the riding model. The final values were  $R_1 = 0.0320$  (against  $F_{hkl}^2$  for 15744 observed reflections with  $I > 2\sigma(I)$ ),  $wR_2 = 0.0690$ ,  $GOF = 1.017$ , and a total number of refined parameters was 793. The SHELXTL PLUS 5.1 package [11] was used. CCDC 621566 contains the supplementary crystallographic data for this article. These data can be obtained free of charge via [www.ccdc.cam.ac.uk/data\\_request/cif](http://www.ccdc.cam.ac.uk/data_request/cif), or by emailing [data\\_request@ccdc.cam.ac.uk](mailto:data_request@ccdc.cam.ac.uk).

## RESULTS AND DISCUSSION

It is known [12] that compositions and structures of tetrahalcogenafulvalene halomercurates obtained by electrocrystallization depend on solvent, temperature, composition and concentration of a supporting electrolyte. Dissociation and complex formation of halomercurate salts, and, consequently, a set of halomercurate ions in solution are defined by solvent and temperature. It was shown that the use of five-percent EtOH/PhCl as a solvent and the  $HgI_2/Bu_4NHgI_3$  electrolyte in the electrochemical synthesis of iodomercurates of BETS [13], EDT-TTF [7,14] and EDT-DTDSF [15] results in the formation of

compounds of  $(\text{Donor})_4\text{Hg}_3\text{I}_8$  stoichiometry. Among them,  $(\text{EDT-DTDSF})_4[\text{Hg}_3\text{I}_8]$  shows a metallic behavior of the temperature dependence of conductivity with the temperature decrease [15],  $(\text{BETS})_4[\text{Hg}_3\text{I}_8]$  undergoes a metal-insulator transition [13], and  $(\text{EDT-TTF})_4[\text{Hg}_3\text{I}_8]_{1-x}$  undergoes a metal-superconductor transition [7,14]. BDA-TTP iodomercures were synthesized in similar conditions. However, the composition of the products of electrochemical oxidation of BDA-TTP was found to be different. At the beginning, we observed the growth of the crystals of the  $(\text{BDA-TTP})_6\text{Hg}_4\text{I}_{10.34}$  salt (**2**), which is characterized by the  $\text{HgI}_2/[\text{HgI}_3]^- = 0.71$  ratio. The structure and the properties of the salt were described in [9]. When the crystals of **2** were removed from the electrode, which was then put back in the cell, the crystals of **1** formed on it. The composition of the products and the sequence of their formation were similar in the syntheses performed at constant current  $I = 0.5 \mu\text{A}$  and  $I = 0.15 \mu\text{A}$ . A consequent formation of **2** and **1** could be due to the changes in reagent concentrations during the electrochemical synthesis or/and the differences in conductivities of crystals of **1** and **2**. Generally [16], when tetrahalcogenafulvalenes are electrooxidized in solution containing two or more different anions, the crystals of highest conducting compounds grow on an anode. Room-temperature measurements of conductivities of **1** and **2** afforded the same value  $\sigma = 2 \text{ S} \cdot \text{cm}^{-1}$ . This implies that the sequence of the formation of **1** and **2** is due to the changes in reagent concentrations during the electrochemical synthesis. The increase in the initial ratio of the supporting electrolyte components,  $\text{HgI}_2/[\text{HgI}_3]^-$ , to 0.72 results in the formation of salt **2** only, and the crystals of **1** do not form.

Crystal structure of **1** was determined at 100 K. The independent part of the unit cell involves four crystallographically nonequivalent BDA-TTP radical cations (O, A, B, C) and the  $[\text{Hg}_2\text{I}_6]^{2-}$  anion, so that formal charge on each radical cation is  $+0.5 e$ . The crystal packing of **1** is specified by the alternation of the iodomercure layers along the  $c$  axis and the BDA-TTP radical cation layers parallel to the  $ab$  plane (Fig. 1). The BDA-TTP radical cations are nonplanar, only the central  $\text{C}_4\text{S}_4$  fragment being planar. In cations A, B, C, both six-membered BDA-TTP cycles are characterized by chair conformation, while in cation O, one of the six-membered cycles has boat conformation. The radical cations are packed in stacks in the  $\dots\text{OABCCBAO}\dots$  sequence, the molecules in the stacks being shifted in the opposite directions with respect to each other along the longer molecular axis. The structure of the radical cation layer of **1** is shown in Figure 2. The shortened  $\text{S}\dots\text{S}$  distances of  $3.301(2)$ – $3.590(2)$  Å were found in the layer. Such contacts are formed both inside and between the stacks. The packing

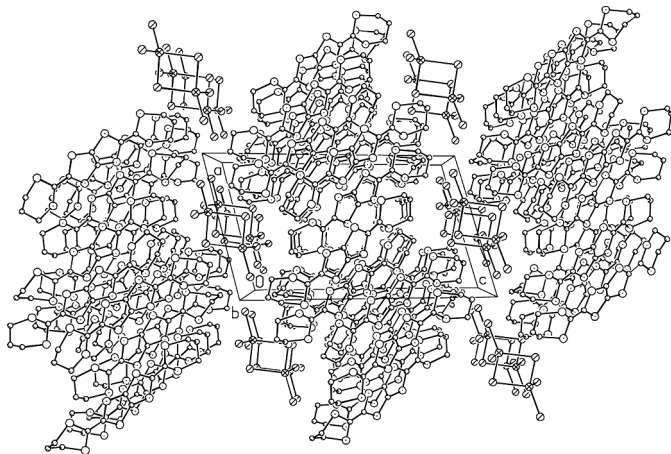


**FIGURE 1** Total packing pattern of **1** along *b* axis.

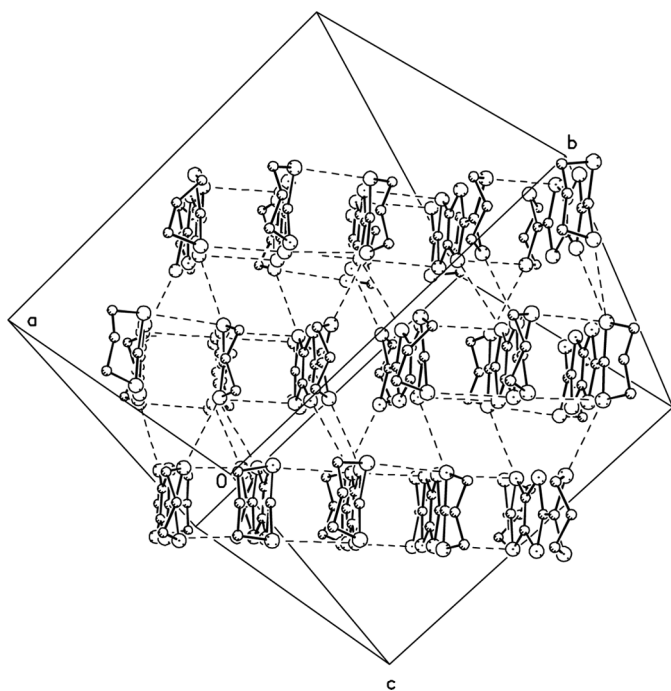


**FIGURE 2** Structure of cation layer in **1**.

mode of the radical cations in the organic layer found in the structure of **1** can be attributed to the so-called  $\beta$ -type, which is often observed in conducting BEDT-TTF salts [17].

The iodomercurate layers of **1** are built of dimeric  $[\text{Hg}_2\text{I}_6]^{2-}$  anions. The mercury atoms in the  $[\text{Hg}_2\text{I}_6]^{2-}$  dimer have a distorted tetrahedral configuration of the Hg-I bonds (see Fig. 1). The Hg-(I bridging) bond lengths are within  $2.8607(4) \div 2.9142(4)$  Å, those of Hg-(I terminal) are  $2.6954(4) \div 2.7233(4)$  Å, the bond lengths of both types being quite close to the lengths of the corresponding Hg-I bonds in the  $[\text{Hg}_2\text{I}_6]^{2-}$  anion at 90 K of  $(\text{EDT-DTDSF})_4\text{Hg}_3\text{I}_8$  [15] ( $2.85 \div 2.92$  и  $2.71 \div 2.73$  Å, respectively). The distance between the Hg atoms in the  $[\text{Hg}_2\text{I}_6]^{2-}$  anion in **1** is appreciably longer ( $4.0939(3)$  Å) than that in  $(\text{EDT-DTDSF})_4\text{Hg}_3\text{I}_8$  ( $3.94$  Å).

It is of interest to compare the crystal structures of **1** and **2** [9] with that of the previously synthesized bromomercurate analog of **1** of the  $(\text{BDA-TTP})_4\text{Hg}_2\text{Br}_6$  composition (**3**) [9]. In these structures, the radical cations form stacks with the arrangement characteristic of  $\beta$ -type structures. The structural motif of the conducting stack of **1** resembles that of **3** (see Fig. 3). In the structures of both compounds, the stacks are divided into tetramers, inside which the radical cations are zigzag shifted by a distance approximately equal to the C=C bond length along the longer molecular axis. The longitudinal shifts between the tetramers are essentially larger and correspond to the tetrathiapentylene bicycle width. In both salts, the radical cations inside the tetramers are linked by S...S contacts shorter than the sum of van-der-Waals radii. There are no short intermolecular S...S contacts between the tetramers in the stack. The conducting layers of **1** and **3** differ in a number of shortened S...S contacts between the radical cations from the

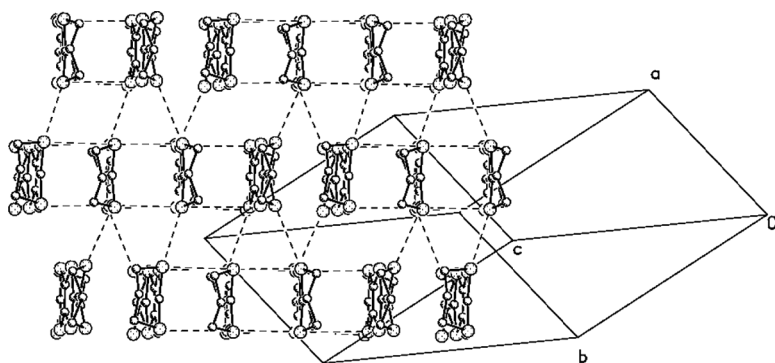


**FIGURE 3** Structure of cation layer in **3**.

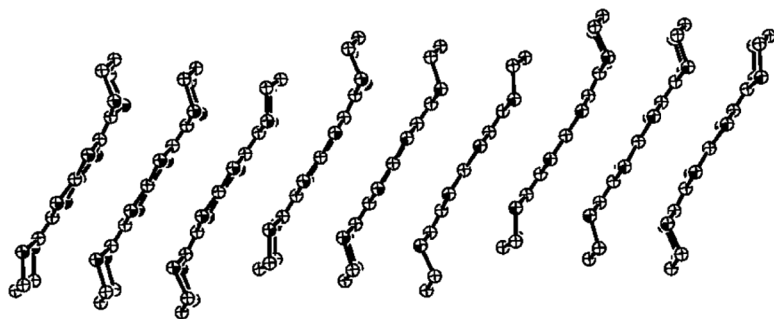


**FIGURE 4** Structure of donor chain in **2**.

neighboring stacks. In **1** four such contacts are per each radical cation, while in **3** there are only three ones.

In the structure of **2** in contrast to those of **1** and **3**, the stacks are divided into triads, all radical cations being shifted along the longer molecular axis to the same direction rather than in a zigzag manner (Fig. 4). There are no shortened S...S contacts inside the stack, and a number of shortened S...S contacts with the radical cations from the neighboring stacks per one radical cation is higher than in **1** and varies from five to six.

The above considered features of the crystal structures of **1–3** were found at low temperatures (100 and 120 K) rather than at room temperature. Nevertheless, they correlate with electroconducting properties studied at temperatures higher than 120 K. The room-temperature values of conductivity of all three compounds are almost similar being equal to  $1\text{--}2 \text{ S} \cdot \text{cm}^{-1}$ . **1–3** exhibit a semiconducting behavior of the temperature dependence of resistivity upon cooling (Fig. 5) with the values of activation energy  $E_a = 0.17, 0.05$ , and  $0.31 \text{ eV}$  (at  $T = 210 \div 293 \text{ K}$ ), which decrease in a strict succession with the increasing number of shortened interstack S...S contacts per one radical cation in each structure. The resistivity data for **1** taken down to 140 K (Fig. 5) show slight changes in the slope of  $\lg R_T/R_{300\text{K}}$  vs.  $1/T$  curve in two points, namely, near 180 and 207 K, the activation energy being equal to  $0.24 \text{ eV}$  within  $207 \div 180 \text{ K}$  and reverting to the initial value  $0.17 \text{ eV}$  below 180 K.

The ESR spectroscopy is a highly sensitive technique for the study of fine differences in the structures of radical cation layers. **1** exhibits the ESR spectrum typical for organic radical cation salts, which consists of a singlet line. The linewidth ( $\Delta H_{\text{pp}}$ ) and  $g$ -value change upon crystal rotating in magnetic field. The  $g$ -values vary from 2.0036 to 2.0095. The linewidths change within  $16.1 \div 18.9 \text{ G}$ . The ESR line

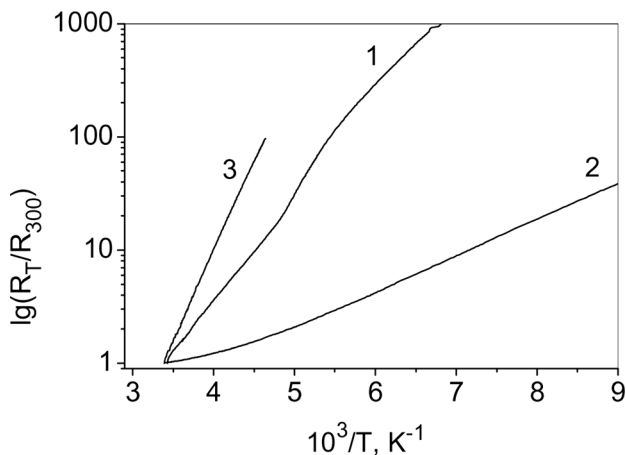


**FIGURE 5** Dependence of logarithm of relative resistivity on inverted temperature for **1**, **2** and **3**.

shape remains almost a Lorentzian one upon crystal rotation, the above to below peak ratio ( $A/B$ ) does not exceed 1.1. Though all the salts **1–3** have the  $\beta$ -like packing of the cation layer near 100 K, the room-temperature ESR linewidth range for **1** is approximately two times larger than those for **2** and **3** [9] and is quite similar to those of BEDT-TTF-based synthetic metals of the  $\beta$ -type packing [2]. The  $\Delta H_{pp}$  for **2** and **3** (6.5–9.5 G and 5.0–8.0 G, respectively) are close to those of the  $\beta'$ -phase of BEDT-TTF salts with a strongly dimerized structure, low conductivity ( $0.01 \text{ S cm}^{-1}$ ), and the Bonner-Fisher behavior of ESR spin susceptibility.

Figure 6 shows the temperature dependences of linewidth  $\Delta H_{pp}$ ,  $g$ -factor and relative spin susceptibility for **1**. The ESR linewidth decreases with temperature as it derives from the Elliot dependence for conducting compounds [2]. However, there is a certain peculiarity in the character of a monotonic dip of the linewidth near 165 K and the value of  $g$ -factor grows namely in this temperature range. The decrease of relative spin susceptibility with temperature suggests an activation character of the dependence of susceptibility similarly to that for **3** [9], which is described by the following expression:

$$\chi \sim C/T^* \exp(-\Delta/T) \quad (1)$$

where  $\Delta$  is an activation energy. The analysis of  $\ln(\chi \cdot T)$  as a function of  $1/T$  (Fig. 7) reveals the changes in the slope of the curve near 183 K. The value of activation energy calculated from the high-temperature

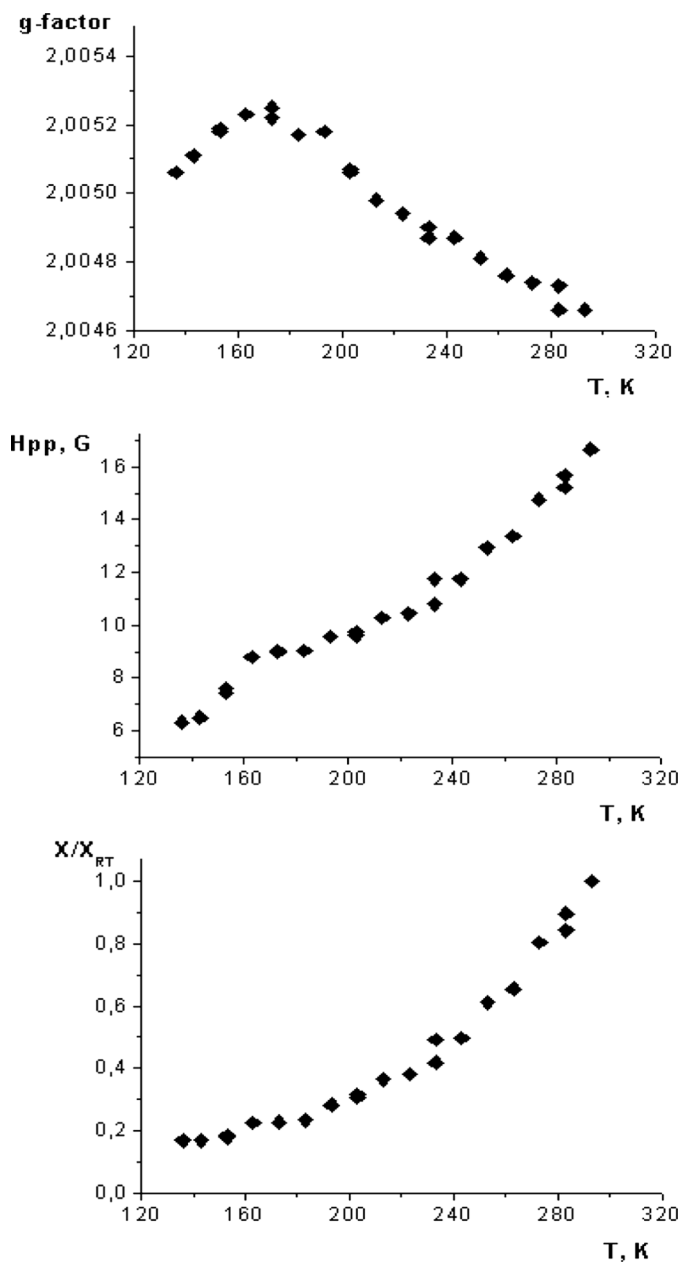


**FIGURE 6** Temperature dependences of g-factor, linewidth  $\Delta H_{pp}$  and relative spin susceptibility  $\chi/\chi_{RT}$  of ESR spectra for **1**.

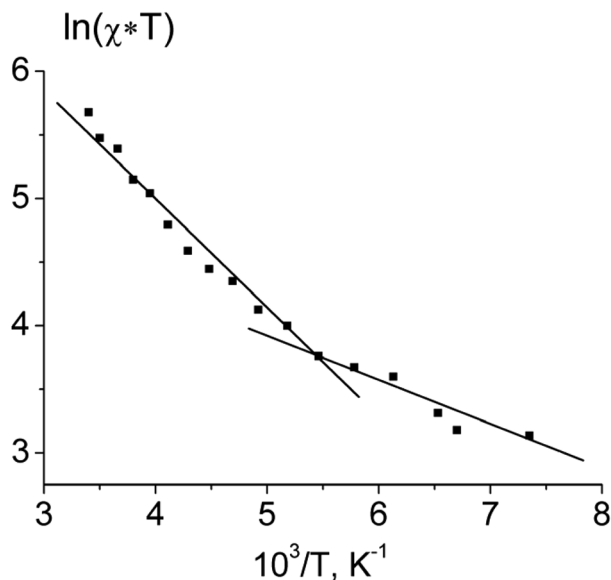


**FIGURE 7** Dependence of  $\ln(\chi \cdot T)$  as a function of inverted temperature for **1** at random crystal orientation.

portion of  $\ln(\chi \cdot T)$  as a function of  $1/T$  is  $\Delta_1 = 0.96 \cdot 10^3 \text{ K}$ , and that calculated from the low-temperature portion is  $\Delta_2 = 0.34 \cdot 10^3 \text{ K}$ . The features of temperature dependences of  $g$ -factor and peak-to-peak linewidth observed at 165–183 K as well as the change in the slope of the curve  $\ln(\chi \cdot T)$  vs.  $1/T$  allow us to assume certain rearrangement in the structure of the radical cation layer.

## CONCLUSION

A new conducting radical cation salt based on a relatively new donor BDA-TTP,  $(\text{BDA-TTP})_4\text{Hg}_2\text{I}_6$ , has been synthesized and characterized. This radical cation salt adopts the  $\beta$ -like packing motif found in other BDA-TTP radical cation salts [8,9]. At 100 K the BDA-TTP donor molecule network consists of stacks, in which each radical cation forms four short interstack  $\text{S} \dots \text{S}$  contacts, the conducting layers being separated by sheets formed by dimeric  $[\text{Hg}_2\text{I}_6]^{2-}$  anions. The title compound is a semiconductor with room-temperature conductivity of  $2 \text{ S} \cdot \text{cm}^{-1}$ . The room-temperature ESR linewidths are within 16.1–18.9 G, which are close to the values characteristic of  $\beta$ -type BEDT-TTF salts and two times higher than those of other BDA-TTP halomercurates [9]. The peculiarities of the temperature dependences

of ESR parameters found at 165–183 K allow one to assume certain rearrangement in the radical cation layers.

## REFERENCES

- [1] Batail, P. (2004). *Chem. Rev.*, **104**, 4887.
- [2] Williams, J. M., *et al.*, (1992). *Organic Superconductors (Including Fullerenes). Syntheses, Structure, Properties, and Theory*. Prentice Hall: Englewood Cliffs, New Jersey.
- [3] Lyubovskaya, R. N., Dyachenko, O. A., & Lyubovskii, R. B. (1993). *Synth. Met.*, **55–57**, 2899.
- [4] Lyubovskaya, R. N., Zhilyaeva, E. I., Pesotskii, S. I., Lyubovskii, R. B., Atovmyan, L. O., Dyachenko, O. A., & Takhirov, T. G. (1987). *Pis'ma v JETP*, **46**, 149. [*JETP Lett.*, **46**, 189 (Engl.Transl.)].
- [5] Lyubovskaya, R. N., Lyubovskii, R. B., Shibaeva, R. P., Aldoshina, M. Z., Goldenberg, L. M., Rozenberg, L. P., Khidekel, M. L., & Shulpyakov, Yu. F. (1985). *Pis'ma v JETP*, **42**, 380. [*JETP Lett.*, **42**, 468, (Engl.Transl.)].
- [6] Zhilyaeva, E. I., Bogdanova, O. A., Lyubovskaya, R. N., Lyubovskii, R. B., Pesotskii, S. I., Perenboom, J. A. A. J., Konovalikhin, S. V., Shilov, G. V., Kobayashi, A., & Kobayashi, H. (2001). *Synth. Met.*, **120**, 1089.
- [7] Lyubovskaya, R. N., Zhilyaeva, E. I., Torunova, S. A., Mousdis, G. A., Papavassiliou, G. C., Perenboom, J. A. A. J., Pesotskii, S. I., & Lyubovskii, R. B. (2004). *J. Phys. IV France*, **114**, 463.
- [8] Yamada, J., Akutsu, H., Nishikawa, H., & Kikuchi, K. (2004). *Chem. Rev.*, **104**, 5057.
- [9] Zhilyaeva, E. I., Flakina, A. M., Lyubovskaya, R. N., Fedyanin, I. V., Lyssenko, K. A., Antipin, M. Yu., Lyubovskii, R. B., Yudanov, E. I., & Yamada, J. (2006). Synthesis, crystal structures and properties of new radical cation salts based on some tetrathiapentalene derivatives with halogenomercurate anions, *Synth. Met.*, doi:10.1016/j.synthmet.2006.06.001.
- [10] Goggin, P. L., King, P., McEwan, D. M., Tayler, G. E., Woodward, P., & Sandstrom, M. (1982). *J. Chem. Soc., Dalton Trans.*, **5**, 875.
- [11] Sheldrick, G. M. (1999). SHELXTL v. 5.10, Structure Determination Software Suite. Bruker AXS, Madison, Wisconsin, USA.
- [12] Lyubovskaya, R. N., Aldoshina, M. Z., Goldenberg, L. M., & Zhilyaeva, E. I. (1991). *Synth. Met.*, **41–43**, 2143.
- [13] Bogdanova, O. A., Gritsenko, V. V., Dyachenko, O. N., Zhilyaeva, E. I., Kobayashi, A., Kobayashi, H., Lyubovskaya, R. N., Lyubovskii, R. B., & Shilov, G. V. (1997). *Chem. Lett.*, **675**.
- [14] Zhilyaeva, E., Torunova, S., Lyubovskaya, R., Mousdis, G., Papavassiliou, G., Perenboom, J., Pesotskii, S., & Lyubovskii, R. (2004). *Synth. Met.*, **140**, 151.
- [15] Zhilyaeva, E. I., Kovalevskiy, A. Yu., Torunova, S. A., Mousdis, G. A., Lyubovskii, R. B., Papavassiliou, G. C., Coppens, P., & Lyubovskaya, R. N. (2005). *Synth. Met.*, **150(3)**, 245.
- [16] Kathirgamonathan, P., Muckklejohn, S. A., & Rosseinsky, D. R. (1979). *J. Chem. Soc. Chem. Commun.*, **2**, 86.
- [17] Mori, T. (1998). *Bull. Chem. Soc. Jpn.*, **71**, 2509.